Structural Aspects of the Allosteric Inhibition of Fructose-1,6-bisphosphatase by AMP: The Binding of Both the Substrate Analogue 2,5-Anhydro-D-glucitol 1,6-Bisphosphate and Catalytic Metal Ions Monitored by X-ray Crystallography[†,‡]

Vincent Villeret,[§] Shenghua Huang,[§] Yiping Zhang,[||] and William N. Lipscomb*[,§]

Gibbs Chemical Laboratory, Harvard University, 12 Oxford Street, Cambridge, Massachusetts 02138, and Syntex Discovery Research, 3401 Hillview Avenue, Palo Alto, California 94303

Received December 15, 1994; Revised Manuscript Received January 27, 1995[⊗]

ABSTRACT: The crystal structures of the T form pig kidney fructose-1,6-bisphosphatase (EC 3.1.3.11) complexed with AMP, the substrate analogue 2,5-anhydro-D-glucitol 1,6-bisphosphate (AhG-1,6-P_2), and Mn^{2+} at concentrations of 5, 15, 100, and 300 μM have been determined and refined at resolutions of 2.1−2.3 Å to *R* factors which range from 0.180 to 0.195, respectively. Two metal ions per active site have been identified, one at a binding site of high affinity (metal site 1′), the second in a low affinity site (metal site 2′). The 1-phosphate group of the substrate analogue coordinates to the metal ion at site 1′, but not at site 2′. In these four complexes, the distances between the two metal ions are all within 0.2 Å of 4.3 Å. In the previously determined R form structure of Fru-1,6-Pase complexed with AhG-1,6-P_2 and Mn^{2+}, there are also two metal ions in the active site at metal sites 1 and 2. The metal ion at site 1 is only 0.6 Å displaced from the metal ion at site 1′ in the T form and is also coordinated to the 1-phosphate group of AhG-1,6-P_2. However, the second metal ion is located in two distinct sites which are 1.4 Å apart in the T and R form structures. In the R form the Mn^{2+} at site 2 is coordinated to the 1-phosphate group of the substrate analogue. This metal ion is apparently required to orient the phosphate group for nucleophilic attack at the phosphorus center. We demonstrate here that differences between metal binding sites in the T and R forms are central to a structural explanation for the allosteric inhibition of Fru-1,6-Pase by AMP when two Mn^{2+} or two Zn^{2+} are required for catalytic activity. Upon binding of AMP, the AMP domain (residues 1−200) is rotated 1.9° relative to the FBP domain (residues 200−335). This movement affects the positions of most residues involved in metal binding. Thus in the T form these conformational changes observed for these residues prevent the binding of Mn^{2+} ion at site 2. The metal ion found at site 2′ (T form) is not coordinated to the 1-phosphate group of the substrate, which is no longer well oriented for the nucleophilic attack at the phosphorus center.

Fructose-1,6-bisphosphatase (Fru-1,6-Pase,[1] EC 3.1.3.11) is a key regulatory enzyme in the gluconeogenic pathway (Marcus, 1981; Van Schaftingen & Hers, 1981; Benkovic & deMaine, 1982; Tejwani, 1983; Van Schaftingen, 1987). It converts D-fructose 1,6-bisphosphate (Fru-1,6-P_2) to D-fructose 6-phosphate (Fru-6-P) and inorganic phosphate. The pig kidney enzyme is a tetramer having *D*2 symmetry, with a molecular mass of 146 000 Da (335 amino acids per monomer). Synergistic inhibition of mammalian Fru-1,6-Pases by AMP at an allosteric site and by Fru-2,6-P_2 at the active site (Marcus, 1981; Pilkis et al., 1981; Van Schaftingen & Hers, 1981; Francois et al., 1983; Tejwani, 1983; Van Schaftingen, 1987; Xue et al., 1995) minimizes, especially at low Fru-2,6-P_2 concentrations, a loss of ATP in a futile cycle catalyzed by Fru-1,6-Pase in the gluconeogenic pathway and phosphofructokinase in glycolysis.

Mammalian Fru-1,6-Pases require the presence of divalent metal ions for catalytic activity (Gomori, 1943). The enzyme is activated most efficiently by Mg^{2+} and Mn^{2+}, and also by Zn^{2+} and Co^{2+} (Kirtley & Dix, 1971; Benkovic & deMaine, 1982; Tejwani, 1983). From kinetic and binding experiments in the presence of Mn^{2+}, Zn^{2+}, or Co^{2+}, it is known that Fru-1,6-Pase contains eight divalent cation sites per molecule of enzyme, i.e., two per subunit (Libby et al., 1975; Benkovic et al., 1978a,b). These two sites display different affinities. The terms "structural" and "catalytic" have been the usual convention of referring to the metal ions at the high affinity sites as "structural" metal and the metal ions at the low-affinity sites, which require the presence of the substrate for binding, as "catalytic" metal, even though direct evidence for the function of either metal ion in the catalytic mechanism is not available (Libby et al., 1975; Benkovic et al., 1978a,b; Pontremoli et al., 1978). However, only one Mg^{2+} was identified in the active site at pH 9.5 (Liu & Fromm, 1990; Zhang et al., 1993).

Crystallographic studies of Fru-1,6-Pase and its complexes have yielded T form structures of the Fru-6-P−AMP−Mg^{2+} complex [2.5 Å resolution (Ke et al., 1990a)], the AMP complex [2.5 Å resolution (Ke et al., 1991a)], the Fru-2,6-P_2−AMP−Zn^{2+} complex [2.1 Å resolution (Xue et al.,

[†] This work is supported by NIH Grant GM 06920 (W.N.L.)

[‡] The coordinates have been deposited in the Brookhaven Protein Data Bank (PDB entry codes: 1FPD, 1FPE, 1FPF, 1FPG).

* To whom correspondence should be addressed.

[§] Harvard University.

[||] Syntex Discovery Research.

[⊗] Abstract published in *Advance ACS Abstracts,* March 15, 1995.

[1] Abbreviations: Fru-1,6-Pase, fructose-1,6-bisphosphatase; Fru-1,6-P_2, fructose 1,6-bisphosphate; Fru-2,6-P_2, fructose 2,6-bisphosphate; Fru-6-P, fructose 6-phosphate; AhG-1,6-P_2, 2,5-anhydro-D-glucitol 1,6-bisphosphate; AhM-1,6-P_2, 2,5-anhydro-D-mannitol-1,6-bisphosphate; AMP, adenosine monophosphate; Tris, tri(hydroxymethyl)aminomethane; PEG, poly(ethylene glycol); EDTA, ethylenediaminetetraacetic acid.

0006-2960/95/0434-4307$09.00/0

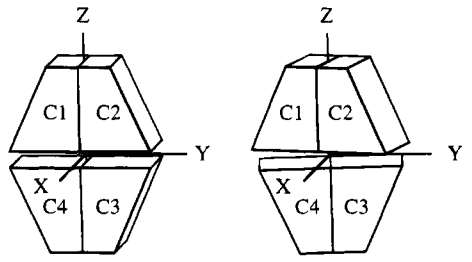

FIGURE 1: Schematic drawing of the Fru-1,6-Pase tetramer in the R and T conformations. The monomers are labeled clockwise as C1, C2, C3, and C4. The quaternary structure of the T and R forms differs by a rotation of 15° of the C3C4 dimer relative to the C1C2 dimer.

1994)], and R form structures of Fru-1,6-Pase complexed with Fru-6-P [2.1 Å resolution (Ke et al., 1991b)], Fru-2,6-P_2 [2.6 Å resolution (Liang et al., 1992a)], Fru-1,6-P_2 (2.5 Å resolution), 2,5-anhydroglucitol 1,6-bisphosphate (AhG-1,6-P_2) (2.6−3.0 Å resolution), and 2,5-anhydromannitol 1,6-bisphosphate (AhM-1,6-P_2) (2.6−3.0 Å) (Zhang et al., 1993), in the presence or absence of metal ions. Two Mn^{2+} or Zn^{2+} ions have been identified in the active site in the presence of AhG-1,6-P_2, the α-anomer analogue of Fru-1,6-P_2. Possible catalytic mechanisms involving two Mn^{2+} or Zn^{2+} have been discussed recently (Zhang et al., 1993).

The four monomers of Fru-1,6-Pase are conventionally labeled clockwise as C1, C2, C3, and C4. The R and T conformations of Fru-1,6-Pase differ by a 15°−17° rotation of the lower dimer C3C4 relative to the upper dimer C1C2 (Figure 1) (Ke et al., 1990, 1991a; Liang et al., 1993; Zhang et al., 1994). AMP binds at an allosteric site, 28 Å away from the active site. During the allosteric transition, a 1.9° rotation of the AMP domain (residues 1−200) relative to the FBP domain (201−335) is observed within the monomer. This movement affects directly the positions of residues which are involved in the coordination of the metal ions. These conformational changes were expected to affect adversely metal binding in the T form structure of Fru-1,6-Pase. However, in the absence of crystallographic evidence for the displacement of the essential metal ions, we could only speculate about the allosteric inhibition of Fru-1,6-Pase (Zhang et al., 1994). The present study was carried out in order to address the effect of the allosteric inhibitor AMP on the binding of the substrate analogue 2,5-anhydroglucitol 1,6-bisphosphate (AhG-1,6-P_2) and Mn^{2+} ions in the active site. We report here the refined structures of Fru-1,6-Pase complexed with AhG-1,6-P_2, AMP, and various concentrations of Mn^{2+} ions (5, 15, 100, and 300 μM). Our results demonstrate how the allosteric transformation affects metal binding in the active site and provide structural evidence relating to the allosteric inhibition of Fru-1,6-Pase by AMP.

MATERIALS AND METHODS

AhG-1,6-P_2 was synthesized according to Hartman and Barker (1965) and was at least 98% pure as shown by ^{31}P NMR spectroscopy. Ultrapure $MnCl_2$ (99.99%) was purchased from Aldrich Chemical Co. Pig kidney Fru-1,6-Pase was purified as described previously (Ke et al., 1990a,b). Crystals of the enzyme complexed with AMP and Fru-6-P were grown following the procedures of Ke et al. (1990b). In order to prepare the different complexes, the crystals were soaked for 3−5 days in a buffer containing 20.0 mM Tris, 20% PEG 3350, 5.0 mM NaN_3, 1.0 mM β-mercaptoethanol, 1 mM AhG-1,6-P_2, and different Mn^{2+} concentrations (5, 15, 100, and 300 μM). The enzyme was crystallized in the space group $P2_12_12$ in which there are two subunits, designated C1 and C2, in the asymmetric unit.

Table 1: Summary of Crystallographic Parameters for data collection, reduction and refinements[a]

	Mn05	Mn15	Mn100	Mn300
a (Å)	61.1	61.1	61.0	61.1
b (Å)	166.4	166.6	166.5	166.5
c (Å)	79.9	80.1	79.9	80.0
total no. of reflections	97 490	89 003	87 818	79 208
no. of unique reflections	42 022	38 697	36 591	36 031
R_{merge}	0.059	0.068	0.069	0.074
resolution (Å)	2.1	2.1	2.2	2.3
completeness (%)	86.7	79.8	81.4	92.7
rms of bond lengths (Å)	0.017	0.018	0.018	0.019
rms of angles (deg)	1.85	1.85	1.83	1.86
R factor	0.191	0.183	0.180	0.195
H_2O (mol/asym unit)	147	156	157	159

[a] Mn05, Mn15, Mn100, and Mn300 refer to Fru-1,6-Pase complexed with AMP−AhG-1,6-P_2 and at Mn^{2+} concentrations of 5, 15, 100, and 300 μM, respectively.

The diffraction data for the complexes referred to as Mn05, Mn15, and Mn100 (see Table 1 legend for abbreviations) were collected using an *R*-axis image plate area detector at Professor Ke's laboratory (School of Medicine, University of North Carolina, Chapel Hill). The diffraction data for the complex referred to as Mn300 were collected on the Siemens multiwire area detector at the Gibbs Laboratory of Harvard University, using the Harvard data collection software (Blum et al., 1987). Data scaling and reduction for this data set were performed using the CCP4 package (CCP4, 1994).

The coordinates of the AMP−Fru-2,6-P_2−Fru-1,6-Pase−Zn^{2+} complex at 2.1 Å resolution (Xue et al., 1994) were used as a starting model for all the complexes. Parameters for AhG-1,6-P_2 and AMP were obtained using the Quanta-Charmm package. In order to rebuilt the structures the O program (Jones et al., 1991) was used. The metal ions were located from (F_o − F_c) difference Fourier maps, contoured at a high level (5σ). Here, F_c represents the calculated structure factor amplitudes obtained using the coordinates of the polypeptide chains of the AMP−Fru-2,6-P_2−Fru-1,6-Pase−Zn^{2+} complex, and F_o represent the observed amplitudes of the various data sets. Solvent molecules which showed well defined density (at least 3σ relative to the mean density) in the (F_o − F_c) map were added to the models. Then positional refinement was carried out using the program X-PLOR (Brunger et al., 1987). In these refinements all charged residues and the Mn^{2+} ions were given a charge of zero throughout the refinements in order to avoid undue bias arising from the long-range Coulomb potential. Those solvent molecules which had *B* values greater than 55 $Å^2$ after the first round of refinement were deleted. Temperature and occupancy factors for the metal ions were refined alternatively, and three refinements of these values were required in order to reach convergence. The statistics for data collection, reduction, and refinements are given in Table 1. We used the RS_FIT option of the O program (Jones et al., 1991) in order to obtain a quantitative evaluation of the fit of the models into the electron density maps. The fit is

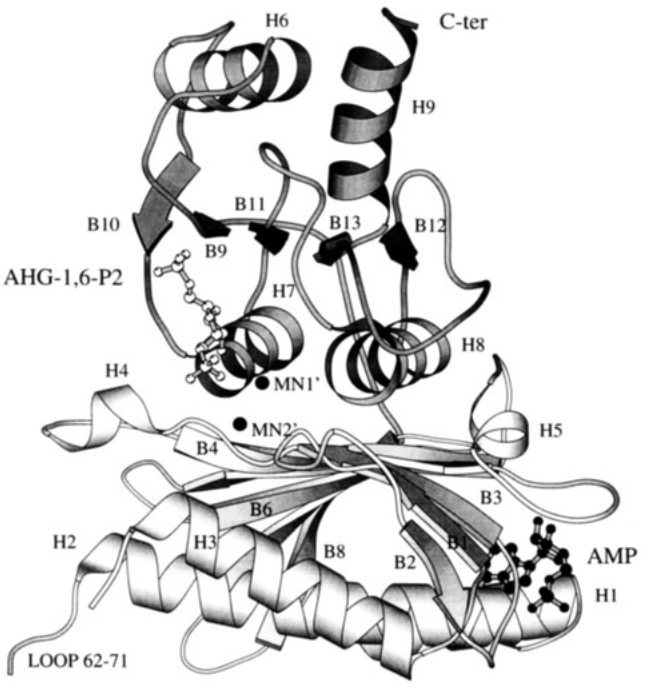

FIGURE 2: Ribbon representation of the Fru-1,6-Pase monomer. AhG-1,6-P_2 and AMP ligands are represented in ball-and-stick mode in their respective binding sites which are 28 Å apart. The two metal ions 1′ and 2′ are labeled MN1′ and MN2′, and are located at the interface between the AMP domain (colored in white-gray) and the FBP domain. The secondary structures are also labeled. The loop between residues 62 and 71 is poorly defined in the electron density map and has not been included to the model. This picture has been generated using MOLSCRIPT (Kraulis, 1991).

very good for all four complexes: only 2−4% of the residues in each monomer (7−12 residues out of 335) have a correlation which is between 0.6 and 0.7. Most of the residues display a correlation greater than 0.9. Analysis of the stereochemistry of the models using the program PROCHECK (Laskowski et al., 1993) shows that 89−90% of the non-glycine residues have ϕ and ψ main chain angles in the most favored regions of the Ramachandran plot. All of the statistics for main-chain and side chains conformations are inside or better than the limits observed for crystallographic structures refined at comparable resolutions (2.1−2.3 Å). Weak electron density is observed for the eight N-terminal residues and also for the 62−71 loop. This loop has been identified as a proteolytically sensitive region for all Fru-1,6-Pases, and has not been included in the refinement of the four structures.

RESULTS

The overall structures of the four complexes resemble the T form structures of Fru-1,6-Pase which were previously reported (Liang et al., 1993; Xue et al., 1994; Zhang et al., 1994). Comparison of the T form structures with the R form Fru-6-P complex (Ke et al., 1991b) shows a rotation between the upper dimer C1C2 and the lower dimer C3C4 of about 15° in the T form (Figure 1). Each monomer has 335 amino acids residues and consists of 9 α helices and 13 β strands. The AMP binding site is located in the AMP domain (residues 9−200) between helices H1 (residues 12−24), H2 (28−50), H3 (72−88) and the eight-stranded β-sheet B1−B8 (which comprises residues from 92 to 200). This allosteric site is 28 Å away from the active site (Figure 2).

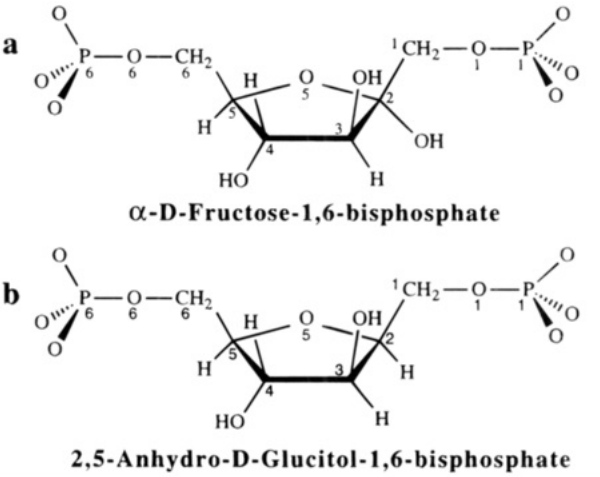

FIGURE 3: Schematic drawings of (a) the α-anomer of Fru-1,6-P_2 and (b) the α analogue AhG-1,6-P_2.

The AMP molecules are well defined in the (F_o − F_c) electron density maps at the 4σ level. In particular, the phosphate oxygens of AMP are hydrogen bonded to the NH groups of Thr-27, Glu-29, Met-30, the NZ of Lys-112, and the OH group of Tyr-113. Also, the hydroxyl oxygen O2′ of the sugar ring interacts with the OH group of Tyr-113 and the NH2 of Arg-140, and the hydroxyl oxygen O3′ interacts with the NH1 of Arg-140. The NH group of the purine base of the AMP molecule is hydrogen bonded to OG1 of Thr-31 and CO of Val-17. In all four complexes, the binding of AMP is identical in monomers C1 and C2. Moreover, the binding of AMP is similar to that observed in the Fru-2,6-P_2−AMP−Fru-1,6-Pase−Zn^{2+} complex (Xue et al., 1994).

(a) Binding of AhG-1,6-P_2 in the Active Sites. The structures of the α-anomer of Fru-1,6-P_2 and its analogue AhG-1,6-P_2 are illustrated in Figure 3. AhG-1,6-P_2 differs from the α-anomer of Fru-1,6-Pase in that the hydroxyl group on C2 (which is required for catalysis) is replaced by a hydrogen atom. The electron density for the substrate analogue AhG-1,6-P_2 is well defined in the (F_o − F_c) difference maps and is at least four times the average background density in the two active sites of each of the four complexes (Figure 4).

The active site can be divided into three regions: the 6-phosphate binding region, the sugar ring binding region, and the 1-phosphate binding region which also includes the metal binding residues. The 6-phosphate and α-methylene D-fructofuranose ring of AhG-1,6-P_2 are identically bound in the two active sites in the asymmetric unit (monomers C1 and C2) in all four complexes. The 6-phosphate oxygen forms hydrogen bonds with side chain OH groups of Tyr-215, Tyr-244, and Tyr-264, with NH2 of Asn-212, all from the same monomer, and with NH1 of Arg-243 from the adjacent monomer. The ester oxygen O6 of the 6-phosphate group is hydrogen bonded to side chain NZ of Lys-274. Three hydrogen bonds stabilize the sugar ring in the active site: between oxygen O5 and side chain NZ of Lys-274 (which forms a bifurcated hydrogen bond to oxygens O6 and O5), and between the backbone amide group of Met-248 which forms a bifurcated hydrogen bond to the hydroxyl oxygens O3 and O4. All of these interactions are summarized in Table 2.

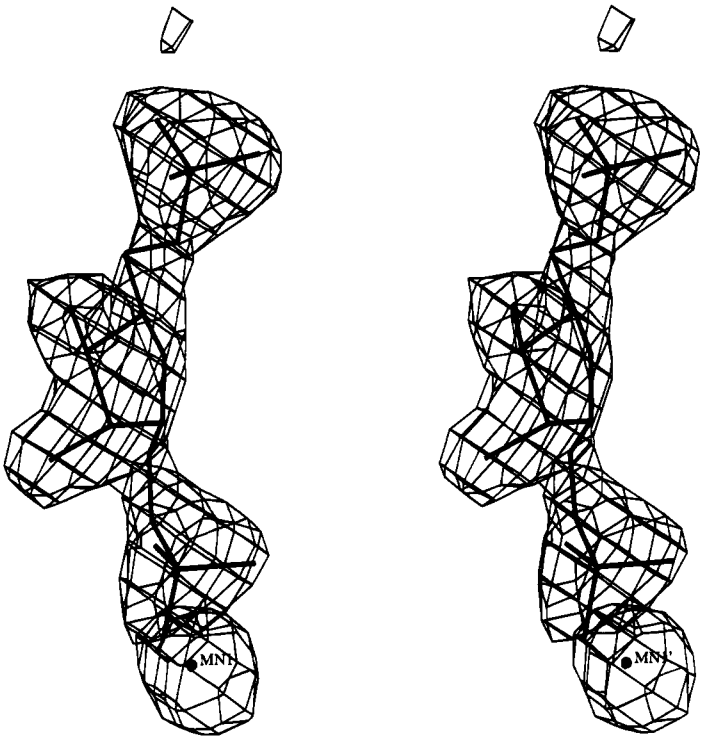

FIGURE 4: Model of AhG-1,6-P_2 built into the electron density in the ($F_o - F_c$) map calculated by omitting the substrate analogue and metal ions. The F_o used in this map are the observed amplitudes of the Mn15 complex. The map is contoured at the 4σ level. Density is also shown of the metal ion at site 1'. The 6-phosphate group is at the top and the 1-phosphate group is at the bottom of the picture.

Table 2: Summary of Interactions of Active Site Residues with Substrate Analogue or Metal Ions[a]

(a) Interactions between AhG-1,6-P_2 and Active Site Residues

atoms	C1[a]	C2[a]
Gly-122 NH	O11[c]	O11, O1
Ser-123 NH		O12
Asn-212 NH2	O22	O22
Tyr-215 OH	O23	O23
Arg-243 NH1[b]	O21	O21
Tyr-244 OH	O22	O22
Met-248 NH	O3, O4	O3, O4
Tyr-264 OH	O23	O23
Lys-274 NZ	O5, O6	O5, O6
Arg-276 NH2	O13	

(b) Interactions between Metal Ions and Active Site Residues

Atoms	C1, C2
Glu-97 OE1	MN2'[d]
Glu-97 OE2	MN1'
Glu-98 OE1	MN2'
Asp-118 OD1	MN2'
Asp-118 OD2	MN1'
Leu-120 OH	MN2'
Asp-121 OD1	MN1'
Glu-280 OE1	MN1'
AhG-1,6-P_2 O11	MN1'

[a] C1 and C2 refer to the two monomers in the asymmetric unit. [b] Arg-243 is from the adjacent chain. [c] O1, O11, O12, and O13 are 1-phosphate oxygens; O6, O21, O22, and O23 are 6-phosphate oxygens. [d] MN1' and MN2' refer to the metal ions at binding site 1' and 2', respectively.

It is of particular importance in this study to refer precisely to the 1-phosphate oxygens, in order to illustrate the differences which occur for the interactions of these oxygens with metal ions and active site residues between the T and R form structures. We will refer to the 1-phosphate oxygens (O11, O12, O13) using the following convention: oxygen O11 is defined as the oxygen which is coordinated to Mn^{2+} at the metal binding site of high affinity (metal site 1'). Oxygens O12 and O13 are labeled clockwise starting from oxygen O11 when the substrate analogue is viewed as in Figure 4. The same convention has been used to describe the interactions between the 1-phosphate oxygens, active site residues, and metal ions in the R form complex Fru-1,6-Pase−AhG-1,6-P_2−Mn^{2+} (Zhang et al., 1993).

The 1-phosphate group shows slightly different binding when monomers C1 and C2 are compared. In monomer C1, oxygen O11 of the 1-phosphate is hydrogen bonded to the backbone amide of Gly-122, and oxygen O13 forms a hydrogen bond with the side chain NH2 of Arg-276. No interaction (within 4.0 Å) is found for oxygen O12 or ester oxygen O1. Oxygen O11 is also coordinated to the Mn^{2+} ion located in metal binding site 1' (see below for a description of the metal binding sites). In monomers C2, oxygen O13 of the 1-phosphate group does not interact with Arg-276. Also in monomer C2 oxygens O11 and O1 are now hydrogen bonded to the backbone amide of Gly-122, and oxygen O12 is 3.5−4.0 Å from the backbone amide of Ser-123. This asymmetry of binding observed for the 1-phosphate group in C1 and C2 is illustrated in Figure 5. The 1-phosphate groups have some flexibility, as indicated by the average *B* factors which are 21.7, 26.1, and 50.1 Å^2 for the 6-phosphate groups, sugar rings, and 1-phosphate groups, respectively, in the MN15 complex. Similar values for these groups are observed in the other complexes.

(b) Mn^{2+} Binding Sites. Two metal binding sites were located by analyzing difference Fourier maps at the active sites. One metal site is well defined in the ($F_o - F_c$) maps and is over 9−11 times the average background electron

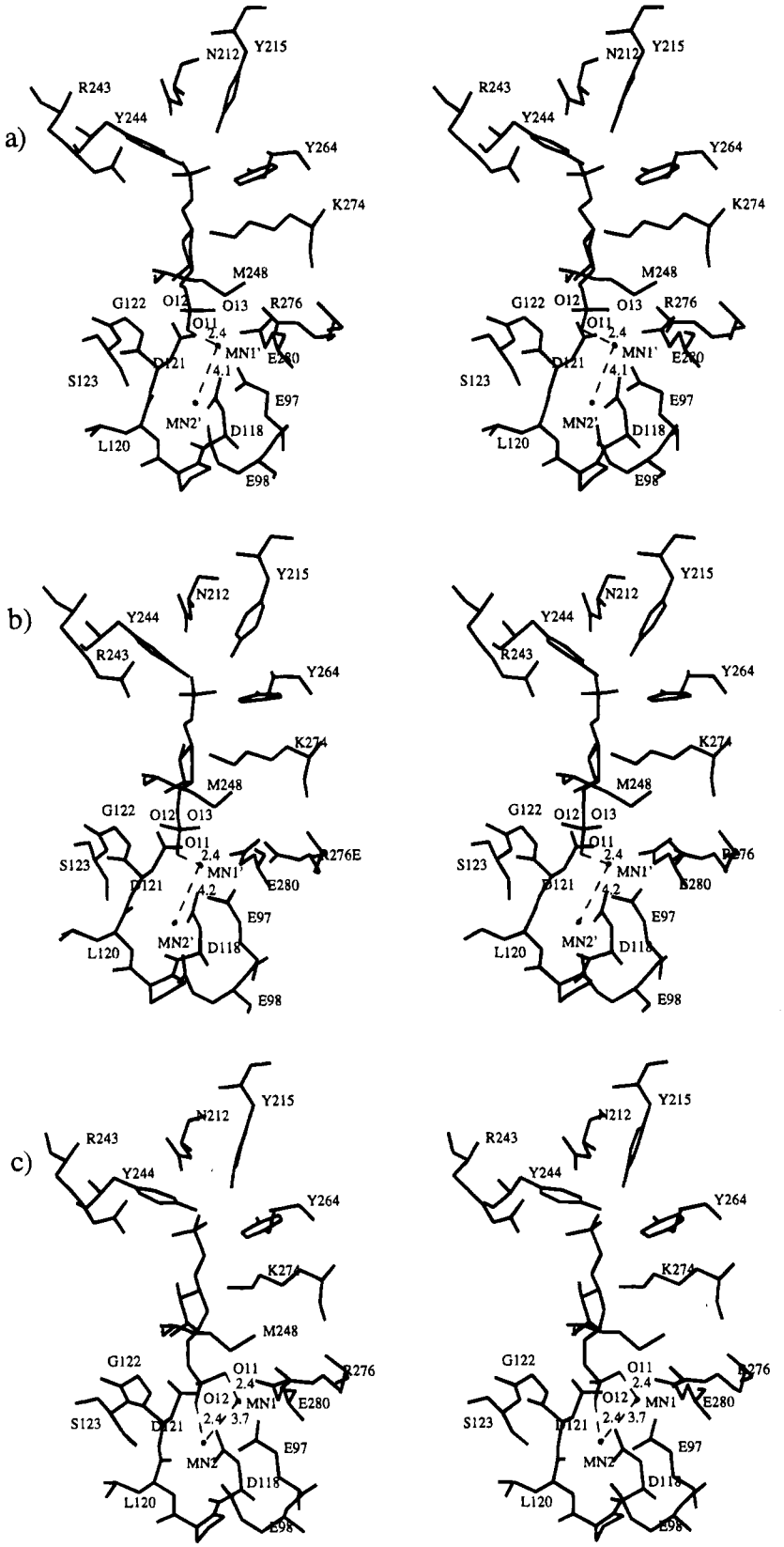

FIGURE 5: Stereoviews of the active site of Fru-1,6-Pase bound to the α analogue AhG-1,6-P_2: (a) in the monomer C1 of the T form structure, in the presence of 300 μM Mn^{2+}; (b) in the monomer C2 of the T form structure, in the presence of 300 μM Mn^{2+}; (c) in the R form structure in the presence of 500 μM Mn^{2+} (Zhang et al., 1993).

density in the four complexes. We will refer to these sites as metal site 1′. The second metal is weakly bound and is 5−8 times the average background electron density. It will be referred to as metal ions at site 2′ (the terms metal site 1 and 2 will be used in the discussion to refer to the two metal binding sites identified in the R form structure of Fru-1,6-Pase complexed with AhG-1,6-P_2). Temperature and occupancy factors for the metal ions are given in Table 3. These values are consistent with the weak electron density observed for the metal ions at sites 2′.

Table 3: Temperature (B) and Occupancy (Q) Factors for Mn^{2+} Ions at Metal Binding Sites 1′ and 2′, in the Monomers C1 and C2 of the Four Complexes

		metal sites MN1′		metal sites MN2′	
complex		B (Å^2)	Q	B (Å^2)	Q
MN05	C1	36.5	0.84	56.5	0.43
	C2	30.4	0.75	49.5	0.38
MN15	C1	39.7	1.0	58.9	0.80
	C2	33.7	0.92	50.1	0.48
MN100	C1	30.2	1.0	55.7	0.85
	C2	29.7	0.92	50.1	0.63
MN300	C1	30.9	0.98	46.3	0.75
	C2	33.2	1.0	44.6	0.69

Mn^{2+} ions at metal site 1′ are bonded by the carboxylate groups of Asp-118, Asp-121, Glu-97, and Glu-280 and coordinated to the oxygen O11 of the 1-phosphate group of AhG-1,6-P_2 (Table 2). The metal binding sites 2′ are defined by the residues Asp-118, Glu-98, Glu-97, and Leu-120. Although the average distance between the metal ions 2′ and the carboxylate groups of Asp-118 is 2.35 Å, distances from ion 2′ to Glu-98, Glu-97, and CO of Leu-120 are larger: 2.9, 2.9, and 2.75 Å for Glu-98, Glu-97, and CO of Leu-120, respectively. Importantly, the 1-phosphate group of the substrate analogue is not coordinated to Mn^{2+} at sites 2′. The average distance between metal 1′ and metal 2′ is 4.2 Å in monomers C1 and 4.4 Å in monomers C2.

Extensive conformational changes are observed for the pig kidney Fru-1,6-Pase when the allosteric transition occurs: upon binding of AMP, relative reorientations of the monomers are observed, which result in a 15° rotation of the C1C2 dimer relative to the C3C4 dimer (Figure 1). Within the monomer, a rotation of 1.9° of the AMP domain (residues 1−200) relative to the FBP domain (residues 201−335) alters the position of some residues involved in metal binding: Glu-97, Glu-98, Asp-118, Leu-120, and Asp-121. These changes were expected to affect adversely metal binding in the T form; however, in the absence of the crystallographic structures of the T form Fru-1,6-Pase complexed with a substrate analogue and metal ions, we could only speculate about the allosteric inhibition of Fru-1,6-Pase (Zhang et al., 1994).

Thus, from our present results, two metal ions are found in the T form complexed with AhG-1,6-P_2 and Mn^{2+}. Crystallographic studies of the R form Fru-1,6-Pase complexed with AhG-1,6-P_2 and Mn^{2+} also reported two metal ions in the active site, at metal binding sites 1 and 2. Metal ion at site 1 in the R form is coordinated to the same residues than metal ion at site 1′ in the T form and is also coordinated to the phosphate oxygen O11. Metal ions 1 and 1′ are 0.6 Å apart when the FBP domains of the T and R forms of Fru-1,6-Pase are superimposed. On the other hand, metal sites 2 (R form) and 2′ (T form) are 1.4 Å apart. These two metal ions are bonded by the same residues, Glu-97, Leu-120, and Asp-118. However, the displacement of residues Glu-97, Asp-118, and Leu-120 observed upon the allosteric transition R → T drastically affects the relative position of metal 2 and 2′ toward the 1-phosphate group of the substrate analogue. The metal ion at site 2 (R form) is also coordinated to one phosphate oxygen (oxygen O12). However, the metal ion at site 2′ (T form) is not similarly coordinated. The phosphate oxygen O12 and metal ion 2′ are 5.3 to 6.5 Å apart, in monomers C1 and C2 of the four T form complexes. Therefore, the 1-phosphate group of the substrate analogue is not coordinated to the low affinity metal ion site in the T form, and, consequently, the 1-phosphate group is not well oriented for nucleophilic attack at the phosphorus center. Our crystallographic studies demonstrate that conformational changes associated with the R to T transition alter the location of the low affinity metal site, which is no longer appropriately positioned to coordinate to the 1-phosphate group for productive catalysis.

DISCUSSION

(a) Binding of AhG-1,6-P_2 in T and R Conformations of Fru-1,6-Pase. Crystallographic studies of the R form structure of Fru-1,6-Pase complexed with substrate, product, and substrate analogues AhG-1,6-P_2 and AhM-1,6-P_2 with or without divalent metal ions (Mn^{2+}, Zn^{2+}, and Mg^{2+}) have been reported previously (Zhang et al., 1993). In solution, the substrate Fru-1,6-P_2 exists mainly in two slowly equilibrating anomeric forms, consisting of about 15% α-anomer and 81% β-anomer (Midelfort et al., 1976). Rapid quench kinetic studies using Mn^{2+} as the activating cation showed that the catalytic reaction proceeds in two phases: first a rapid formation of the product, corresponding to about 18% of the available substrate, followed by a slow reaction which has an apparent rate independent of the enzyme concentration and close to the rate of the nonenzymatic conversion of the β- to α-anomer in solution (Benkovic et al., 1974; Frey et al., 1977). These experiments and the findings that in the crystal structures two Mn^{2+} and Zn^{2+} ions are bound in the presence of AhG-1,6-P_2 and only one ion is bound in the presence of AhM-1,6-P_2 (the analogue of the β-anomer of Fru-1,6-P_2) are consistent with the conclusion that the α-anomer of Fru-1,6-P_2 is the true substrate (Zhang et al., 1993). Thus, the α analogue AhG-1,6-P_2 was chosen for the present study.

AhG-1,6-P_2 is well defined in the electron density maps of both T and R conformations. The binding of the 6-phosphate group and the α-methylene D-fructofuranose ring is nearly identical in the two forms: in the ternary complex AhG-1,6-P_2−Fru-1,6-Pase−Mn^{2+}, the 6-phosphate group is also hydrogen bonded to side chain groups of Tyr-215, Tyr-244, Tyr-264, and Lys-274, NH2 of Asn-212, and the side chain NH1 of Arg-243 from the adjacent monomer. Hydroxyl oxygens O3 and O4 of the sugar ring are hydrogen bonded to the backbone amide of Met-248, and the oxygen O5 is hydrogen bonded to side chain NZ of Lys-274 (Zhang et al., 1993). All of these interactions are also observed in the quaternary complex AMP−AhG-1,6-P_2−Fru-1,6-Pase−Mn^{2+} (Table 2). The residues involved in 6-phosphate and sugar ring binding belong to the FBP domain (residues 200−335) which is well preserved between the T and R conformations. For example, the root mean square (rms) deviation between backbone atoms of the FBP domains of the T and R forms is 0.5 Å.

The binding site of the 1-phosphate group of AhG-1,6-P_2 involves residues of the AMP domain (residues 1−200) which undergo conformational changes during the allosteric transformation. In the ternary complex AhG-1,6-P_2−Fru-1,6-Pase−Mn^{2+} (R form), the main chain NH of Gly-122 forms a bifurcated hydrogen bond to the ester oxygen O1 and 1-phosphate oxygen O12 (Zhang et al., 1993). These interactions act to orient this group into proper position for

activation and catalysis. In the quaternary complex AMP−AhG-1,6-P_2−Fru-1,6-Pase−Mn^{2+}, different interactions are observed for the 1-phosphate oxygens (Table 2). In the T form structure, oxygen O11 is hydrogen bonded to NH of Gly-122 in both C1 and C2, instead of oxygen O12 in the R form. In monomer C2 of the T form, oxygen O12 is close to the backbone amide of Ser-123, but no interaction is observed in monomer C1 for this oxygen. Also the interaction between the ester oxygen O1 and the NH of Gly-122 is found only in monomer C2. As described above, oxygen O13 is hydrogen bonded to Arg-276 in monomer C2 of the T form, but this interaction is not observed in monomer C1. The same asymmetric interaction was observed in the binary complex Fru-1,6-Pase−Fru-1,6-P_2 (R form without metal ion) but not in the ternary complex Fru-1,6-Pase−Fru-1,6-P_2−Mn^{2+}, as a result of the repositioning of the 1-phosphate group which occurs in the R form in the presence of metal ions. It is clear from these complexes that the allosteric transformation which occurs upon binding of AMP at the allosteric site does not affect the binding of the 6-phosphate group and sugar ring in the active site but does affect the binding and orientation of the 1-phosphate group.

(b) Binding of Mn^{2+} ions in T and R Conformations of Fru-1,6-Pase. Various kinetic studies of the binding of divalent metal ions to Fru-1,6-Pase have been reported. For manganese, one metal was bound to each monomer in the absence of substrate, or two metal ions were bound to each monomer in the presence of substrate or its α analogue (Pontremoli et al., 1969; Grazi et al., 1971; Libby et al., 1975; Benkovic et al., 1978b). The enzyme was active only after the second metal ion was bound. On the basis of these kinetic and binding experiments, the four strongly bound metal ions per tetramer of Fru-1,6-Pase are designated as "structural" metal and the second set of four less strongly bound metal ions as "catalytic" metal (Grazi et al., 1971; Libby et al., 1975; Tejwani et al., 1976; Pedrosa et al., 1977; Benkovic et al., 1978a,b; Pontremoli et al., 1979), although both Mn^{2+} ions are required for catalytic activity. Fluorescence studies with formycin 5′-monophosphate (FMP), which inhibits the enzyme, as does AMP, led to the conclusion that catalytic metal ion (which binds to the low affinity site, with a K_d of 14 μM in the presence of AhG-1,6-P_2) is competitive with nucleotide binding at the allosteric site (Scheffler & Fromm, 1986a). Comparison of the crystallographic structure of unliganded Fru-1,6-Pase and that complexed with AMP shows a 1.9° rotation of the AMP domain relative to the FBP domain within a monomer. Changes in positions of metal binding residues between the R and T structures were also reported (Zhang et al., 1994): during the R to T transition, Cα of Glu-97 moves 0.95 Å, Cα of Asp-118 moves 0.63 Å and its side chain OD2 moves 1.85 Å; the carbonyl oxygen of Leu-120 moves 1.01 Å, and finally the Cα and OD2 of Asp-121 move 1.10 and 2.80 Å, respectively. These movements were expected to affect the binding of metal ions in the active site.

Previous crystallographic studies of the catalytic mechanism of Fru-1,6-Pase (Liang et al., 1992b; Zhang et al., 1993) reported two metal binding sites in the ternary R state complex AhG-1,6-P_2−Fru-1,6-Pase−Mn^{2+} (or Zn^{2+}). In this complex the two metal ions are bound by the carboxylate group of Glu-97, Asp-118, and the 1-phosphate group of AhG-1,6-P_2. All of these groups act as bridging bidentate ligands in the R form structure. Other ligands of metal 1 and metal 2 are the carboxylate oxygen OD2 of Glu-280 and the carbonyl oxygen of Leu-120, respectively. If the FBP domains are superimposed, the metal ion at site 1′ in the T form is only 0.6 Å away from the metal ion at site 1 in the R form. Moreover, the metal ions at site 1′ in the T form and site 1 in the R form are bound to the same residues, except that Asp-121 is directly bounded to the metal in the T form, but not in the R form: in this R structure the distance between the carboxylate group of Asp-121 and Mn^{2+} is 2.8 Å. An indication that the Mn^{2+} ion at site 1 or 1′ is strongly bound to the enzyme, in either the T or R form, is that the electron density of the metal is 8−16 times above the average background. This metal ion corresponds to the "structural" metal described on the basis of kinetic and binding experiments.

Coordination of the second metal ion, which is seen at 5−8 times the average background electron density, is drastically affected upon binding of AMP to Fru-1,6-Pase. In the T form structure, the Mn^{2+} ion at site 2′ is bound to Asp-118, Glu-98, Glu-97, and Leu-120 and occupies a different site than does metal 2 in the R form. The distance between the second metal ions in the T and R conformations (sites 2′ and 2) is 1.4 Å after superimposing the FBP domains. The 1-phosphate group coordinates the two metal ions in the R form: oxygen O12 is 2.4 Å away from metal 2, and oxygen O11 is 2.4 Å away from metal 1. Also, in the R form, the position of the 1-phosphate group is stabilized by the hydrogen bond between oxygen O12 and the NH of Gly-122. In the T form, however, the 1-phosphate group coordinates to the metal ion at site 1′ but importantly does not also coordinate to the metal ion at site 2′. Oxygen O11, which is 2.4 Å away from metal 1′, is now hydrogen bonded to NH of Gly-122, and oxygen O12 no longer interacts with Gly-122 (Table 2).

(c) Inhibition of Fru-1,6-Pase upon Binding of AMP. The results from kinetic and binding studies suggested a kinetic model in which each active site binds the first metal ion at the high affinity site, then the substrate Fru-1,6-P_2, and finally the second metal ion at the low affinity site, followed by the hydrolysis of the 1-phosphate group of Fru-1,6-P_2 (Libby et al., 1975; Caparelli et al., 1978; Dudman et al., 1978; Benkovic et al., 1978b). A catalytic mechanism using Mn^{2+} or Zn^{2+} as the activating cation has been discussed previously (Zhang et al., 1993). This mechanism can be summarized as follows (Figure 6): the C2-hydroxyl group of Fru-1,6-P_2 (the missing hydroxyl group in AhG-1,6-P_2) forms an intramolecular hydrogen bond to the ester oxygen O1 of the 1-phosphate group. This oxygen is also hydrogen bonded to NH of Gly-122. A water molecule can be activated by binding to metal ion 2 in a position for in-line nucleophilic attack at the 1-phosphate from the direction opposite to that of the scissile P−O bond. This attack could be facilitated by the side chain of Glu-98, which is 4.5 Å from metal ion 2 and could deprotonate the water molecule. The metal ion 2 could become five-coordinated, or the carbonyl oxygen of Leu-120 could be displaced to preserve the tetrahedral geometry. In addition, a proton could be transferred from the un-ionized side chain carboxyl group of Asp-121 to the substrate ester oxygen O1 directly or through the help of the C2-hydroxyl group of the substrate, thus weakening the P−O bond. A central feature is the positioning of the 1-phosphate group so that it coordinates the two metal ions at sites 1 and 2. If we compare the T and R form structures

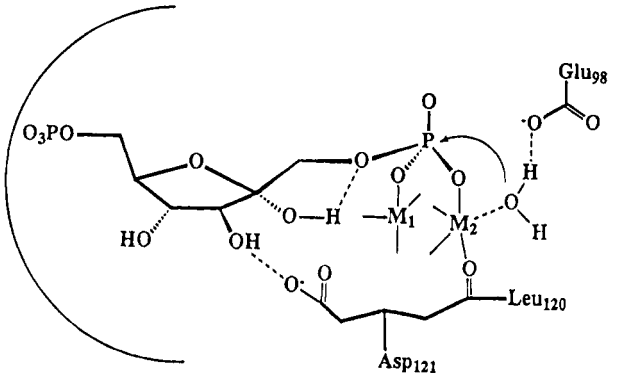

FIGURE 6: Schematic representation of one proposed catalytic mechanism [reproduced from Zhang et al. 1993)] when two metal ions are involved. Bridging ligands are implied by the terminal lines emanating from the metal ions. Proposed nucleophilic attack by oxygen of H_2O or incipient OH^- on the phosphorus of the 1-phosphate may be assisted by proton transfer from this H_2O to Glu-98. Proton transfer to the bridging oxygen O1 may be assisted by Asp-121 and the C2-hydroxyl group.

complexed with Mn^{2+} and AhG-1,6-P_2, it is clear that the metal ion at site 1 or 1′ is still coordinated to the 1-phosphate group of the substrate or substrate analogue. In the T form, the allosteric transformation prevents metal binding at site 2. A second metal ion is weakly bound at metal site 2′ but is no longer coordinated to the 1-phosphate group. Moreover, Asp-121, which is 2.8 Å away from metal 1 in the R form, is coordinated to the metal ion at site 1′ in the T form, such that its carboxyl group is not then available to transfer a proton to ester oxygen O1.

These modifications help to explain the allosteric inhibition of Fru-1,6-Pase by AMP. Our crystallographic results are consistent with the binding sequence in which a "structural" metal binds first at metal site 1, followed by the substrate and finally a second metal ion at site 2. They also support the suggestion that the role of metal ion at site 1, which is a high affinity binding site, is mainly to facilitate the binding of the 1-phosphate group of the substrate and possibly to make the phosphorus atom more susceptible to nucleophilic attack. The metal ion at site 2 would orient the 1-phosphate group and activate the water molecule for nucleophilic attack at the phosphorus center.

We demonstrated here that differences between metal binding sites in the T and R forms are central to a structural explanation for the allosteric inhibition of Fru-1,6-Pase by AMP when two Mn^{2+} or two Zn^{2+} are required for catalytic activity. Upon binding of the allosteric inhibitor AMP, a cascade of structural changes occurs within the monomer, starting from the AMP site: local conformational changes of helices H1 and H2, independent rotations and translations of helices H1, H2, and H3 and loops connecting them. Moreover, the AMP domain (residues 1−200) is rotated 1.9° relative to the FBP domain. Consequently, the position of the residues involved in metal binding and which belong to the AMP domain (Glu-97, Glu-98, Asp-118, Leu-120, and Asp-121) are affected. These modifications of the metal binding residues prevent the binding of Mn^{2+} at site 2; this metal ion is coordinated to the 1-phosphate group of the substrate in the R form Fru-1,6-Pase. On the other hand, the metal ion found at site 2′ in the T form is not coordinated to the 1-phosphate group of the substrate, which is no longer well oriented for the nucleophilic attack at the phosphorus center.

Our current knowledge about the catalysis and allosteric inhibition of Fru-1,6-Pase is therefore more advanced, but it remains unclear how the catalysis can proceed in the presence of Mg^{2+} ions, since only one Mg^{2+} was found in the active site in the presence of AhG-1,6-P_2 (Zhang et al., 1993). A modified catalytic mechanism for Mg^{2+} may not be excluded. More experiments are needed to answer these specific questions regarding the role of Mg^{2+} in the catalytic mechanism of Fru-1,6-Pase.

ACKNOWLEDGMENT

We thank Dr. H. Ke for help in data collection and Dr. M. Nolte for critical reading of the manuscript.

REFERENCES

Benkovic, P. A., Bullard, W. P., deMaine, M. M., Fishbein, R., Scray, K. J., Steffens, J. J., & Benkovic, S. J. (1974) *J. Biol. Chem. 249*, 930−931.
Benkovic, P. A., Frey, W. A., & Benkovic, S. J. (1978a) *Arch. Biochem. Biophys. 191*, 719−726.
Benkovic, P. A., Caperelli, C. A., deMaine, M. M., & Benkovic, S. J. (1978b) *Proc. Natl. Acad. Sci. U.S.A. 75*, 2185−2189.
Benkovic, S. J., & deMaine, M. M. (1982) *Adv. Enzymol. Relat. Areas Mol. Biol. 53*, 45−82.
Blum, M., Metcalf, P., Harrison, S. C., & Wiley, D. C. (1987) *J. Appl. Crystallogr. 20*, 235−242.
Brunger, A. T., Kuriyan, J., & Karplus, M. (1987) *Science 235*, 458−460.
Caperelli, C. A., Frey, W. A., & Benkovic, S. J. (1978) *Biochemistry 17*, 1699−1704.
CCP4. Collaborative Computational Project, Number 4 (1994) *Acta Crystallogr.* D50, 760−763.
Dudman, N. P. B., deMaine, M. M., & Benkovic, S. J. (1978) *J. Biol. Chem. 253*, 5712−5718.
Francois, J., van Schaftingen, E., & Hers, H.-G. (1983) *Eur. J. Biochem. 134*, 269−273.
Frey, W. A., Fishbein, R., deMaine, M. M., & Benkovic, S. J. (1977) *Biochemistry 16*, 2479−2884.
Gomori, G. J. (1943) *J. Biol. Chem. 148*, 139−149.
Grazi, E., Accorsi, A., & Pontremoli, S. (1971) *J. Biol. Chem. 246*, 6651−6654.
Han, P. F., Han, G. Y., McBay, H. C., & Johnson, J., Jr. (1980) *Biochem. Biophys. Res. Commun. 93*, 558−565.
Hartman, F. C., & Barker, R. (1965) *Biochemistry 4*, 1068.
Ikeda, T., Kimura, K., Hama, T., & Tamaki, N. (1980) *J. Biochem. (Tokyo) 87*, 179−185.
Jones, T. A., Zou, J.-Y., Cowan, S. W., & Kjeldgaard, M. (1991) *Acta Crystallogr. A47*, 110−119.
Katajima, S., & Uyeda, K. (1983) *J. Biol. Chem. 258*, 7352.
Ke, H., Zhang, Y., & Lipscomb, W. N. (1990a) *Proc. Natl. Acad. Sci. U.S.A. 87*, 5243−5247.
Ke, H., Thorpe, C. M., Seaton, B. A., Lipscomb, W. N., & Marcus, F. (1990b) *J. Mol. Biol. 212*, 513−539; *214*, 950.
Ke, H., Liang, J.-Y., Zhang, Y., & Lipscomb, W. N. (1991a) *Biochemistry 30*, 4412−4420.
Ke, H., Zhang, Y., Liang, J.-Y., & Lipscomb, W. N. (1991b) *Proc. Natl. Acad. Sci. U.S.A. 88*, 2989−2993.
Kirtley, M. E., & Dix, J. (1971) *Arch. Biochem. Biophys. 147*, 647−652.
Kraulis, P. J. (1991) *J. Appl. Crystallogr. 24*, 946−950.
Krebs, H. A., & Woodford, M. (1965) *Biochem. J. 94*, 436−445.
Laskowski, R. A., MacArthur, M. W., Moss, D. S., & Thornton, J. M. (1993) *J. Appl. Crystallogr. 26*, 283−291.
Liang, J.-Y., Huang, S., Zhang, Y., Ke, H., & Lipscomb, W. N. (1992a) *Proc. Natl. Acad. Sci. U. S. A. 89*, 2404−2408.
Liang, J.-Y., Zhang, Y., Huang, S., Ke, H., & Lipscomb, W. N. (1992b) in *Proceedings of the Robert A. Welch Foundation Conference on Chemical Research 36. Regulation of Proteins by Ligands*, October 26−27, 1992, Houston Texas, pp 57−99.
Libby, C. B., Frey, W. A., Villafranca, J. J., & Benkovic, S. J. (1975) *J. Biol. Chem. 250*, 7564−7573.
Liu, F., & Fromm, H. J. (1990) *J. Biol. Chem. 265*, 7401−7406.

Marcus, F. (1981) in *The Regulation of Carbohydrate Formation and Utilization in Mammals* (Veneziale, C. M., Ed.) pp 269–290, University Park Press, Baltimore, MD.
Midelfort, C. F., Gupta, R. K., & Rose, I. A. (1976) *Biochemistry 15*, 2178–2185.
Nimmo, H. G., & Tipton, K. F. (1975a) *Eur. J. Biochem. 58*, 567–574.
Pedrosa, F. O., Pontremoli, S., & Horecker, B. L. (1977) *Proc. Natl. Acad. Sci. U.S.A. 74*, 2742–2745.
Pilkis, S. J., El-Maghrabi, M. R., Pilkis, J., & Claus, T. (1981) *J. Biol. Chem. 256*, 3619–3622.
Pontremoli, S., Grazi, E., & Accorsi, A. (1969) *Biochem. Biophys. Res. Commun. 37*, 597–602.
Pontremoli, S., Melloni, E., Salamino, F., Sparatore, B., & Horecker, B. L. (1978) *Arch. Biochem. Biophys. 188*, 90–97.
Pontremoli, S., Sparatore, B., Salamino, F., Melloni, E., & Horecker, B. L. (1979) *Arch. Biochem. Biophys. 194*, 481–485.
Racker, E., & Schroeder, E. A. R. (1958) *Arch. Biochem. Biophys. 74*, 326–344.
Scheffler, J. E., & Fromm, H. J. (1986a) *Biochemistry 25*, 6659–6665.
Scheffler, J. E., & Fromm, H. J. (1986b) *Fed. Proc. 45*, 2263.
Tejwani, G. A. (1983) *Adv. Enzymol. Relat. Areas Mol. Biol. 54*, 121–194.
Tejwani, G. A., Pedrose, F. O., Pontremoli, S., & Horecker, B. L. (1976a) *Arch. Biochem. Biophys. 177*, 255–264.
Tejwani, G. A., Pedrosa, F. O., Pontremoli, S., & Horecker, B. L. (1976b) *Proc. Natl. Acad. Sci. U.S.A. 73*, 2692–2695.
Underwood, A. H., & Newsholme, E. A. (1965) *Biochem. J. 95*, 767–774.
Van Schaftingen, E. (1987) *Ad. Enzymol. Relat. Areas Mol. Biol. 59*, 315–395.
Van Schaftingen, E., & Hers, H.-G. (1981) *Proc. Natl. Acad. Sci. U.S.A. 78*, 2861.
Van Tol, A., Black, W. J., & Horecker, B. L. (1972) *Arch. Biochem. Biophys. 151*, 591–596.
Xue, Y., Huang, S., Liang, J.-Y., Zhang, Y., & Lipscomb, W. N. (1994) *Proc. Natl. Acad. Sci. U.S.A. 91*, 12482–12486.
Zhang, Y., Liang, J.-Y., Huang, S., Ke, H., & Lipscomb, W. N. (1993) *Biochemistry 32*, 1844–1857.
Zhang, Y., Liang, J.-Y., Huang, S., & Lipscomb, W. N. (1994) *J. Mol. Biol. 244*, 609–624.

BI942882I